Letter of Intent to the Jefferson Lab Program Advisory Committee

Measuring the Charged Pion Polarizability in the $\gamma\gamma \to \pi^+\pi^-$ Reaction

R. Miskimen†, A. Mushkarenkov
University of Massachusetts, Amherst, MA

D. Lawrence, E. Smith
Jefferson Laboratory, Newport News, VA

† contact person: miskimen@physics.umass.edu

1 Abstract

This Letter of Intent presents our plan to make a measurement of the charged pion polarizability $\alpha_\pi - \beta_\pi$ through measurements of $\gamma\gamma \to \pi^+\pi^-$ cross sections using the GlueX detector in Hall D. The charged pion polarizability ranks among the most important tests of low-energy QCD presently unresolved by experiment . Analogous to precision measurements of $\pi^0 \to \gamma\gamma$ that test the intrinsic odd-parity (anomalous) sector of QCD, the pion polarizability tests the intrinsic even-parity sector of QCD.

2 Introduction

Electromagnetic polarizabilities are fundamental properties of composite systems such as molecules, atoms, nuclei, and hadrons [Ho90]. Whereas magnetic moments provide information about the ground state properties of a system, polarizabilities provides information about the excited states of the system. For atoms the polarizabilities are of order the atomic volume. For hadrons the polarizabilities are much smaller than the volume, typically of order $10^{-4} fm^3$, because of the much greater stiffness of the QCD force as compared to the electromagnetic force. Measurements of hadron polarizabilities provide an important test point for effective field theories, dispersion theories, and lattice calculations.

Hadron polarizabilities are best measured in Compton scattering experiments, where in the case of nucleon polarizabilities one looks for a deviation of the cross section from the prediction of Compton scattering from a structureless Dirac particle. The electric and magnetic polarizabilities of the proton, α_p and β_p, have been measured in Compton scattering experiments at Mainz and other laboratories [Sc05], and in the near future it can be expected that neutron polarizabilities will be extracted from Compton scattering experiments on the deuteron and ^3He.

Because a free pion target doesnt exist, the measurements to date of the charged pion polarizability have been plagued by experimental and theoretical uncertainties. This letter of intent presents a plan to make a new measurement of the charged pion polarizability by measurement of $\gamma\gamma \to \pi^+\pi^-$ cross sections using the GlueX detector in Hall D.

3 Theoretical predictions for the charged pion polarizability

Theory for the the charged pion polarizability results directly from the original formulation of chiral perturbation theory (ChPT) by Gasser and Leutwyler [Ga84]. This lagrangian is invariant under the transformation $\phi_i \to -\phi_i$, where ϕ_i represents the eight Goldstone boson fields, and has the feature that it doesn't allow transitions between even and odd numbers of mesons. For example, the transition $\pi^0 \to \gamma\gamma$ is not allowed at leading order $O(p^4)$ [Ho92]. For this reason the lagrangian must be augmented by the Wess-Zumino-Witten anomaly [We71]. Recently the PRIMEX experiment at JLab made a precision test of the intrinisic *odd-parity* (anomalous) sector of low-energy QCD by measuring the radiative width for $\pi^0 \to \gamma\gamma$ [La11]. A measurement of the charged pion polarizability probes the intrinsic *even-parity* sector of QCD.

PCAC and leading order $O(p^4)$ chiral perturbation theory (ChPT) [Do89] both predict that the electric and magnetic polarizabilities of the charged pion (α_π and β_π) are related to the charged pion weak form factors F_V and F_A in the decay $\pi^+ \to e^+\nu\gamma$

$$\alpha_\pi = -\beta_\pi = \frac{4\alpha_{EM}}{m_\pi F_\pi^2}(L_9^r + L_{10}^r) \propto \frac{F_A}{F_V} \tag{1}$$

where L_9^r and L_{10}^r are low energy constants in the Gasser and Leutwyler effective Lagrangian [Ga84], and α_{EM} is the fine structure constant. Using recent results from the PIBETA collaboration for F_A and F_V [By09], the $O(p^4)$ ChPT prediction for the charged pion electric and magnetic polarizabilities is given by

$$\alpha_\pi = -\beta_\pi = 2.78 \pm 0.1 \times 10^{-4} fm^3 \tag{2}$$

The $O(p^6)$ corrections are predicted to be relatively small [Bu96,Ga06], giving the following results,

$$\alpha_\pi - \beta_\pi = 5.7 \pm 1.0 \times 10^{-4} fm^3 \tag{3}$$

$$\alpha_\pi + \beta_\pi = 0.16 \pm 0.1 \times 10^{-4} fm^3 \tag{4}$$

Dispersion relations have also been used to find α_π and β_π, where $\gamma\gamma \to \pi^+\pi^-$ data are used to fix the dispersion integrals. Fitting $\gamma\gamma \to \pi^+\pi^-$ data from threshold up to 2.5 GeV, Fil'kov et. al. [Fi06] found that

$$\alpha_\pi - \beta_\pi = 13.0 + 2.6 - 1.9 \times 10^{-4} fm^3 \tag{5}$$

$$\alpha_\pi + \beta_\pi = 0.18 + 0.11 - 0.02 \times 10^{-4} fm^3 \tag{6}$$

which is in disagreement with ChPT.

Pasquini et al. [Pa08] examined the Fil'kov calculation in detail, and noted that the energy extrapolations used by Fil'kov below and above meson resonances leave considerable room for model dependence. When the basic requirements of dispersion relations are taken into account , Pasquini et al. found that dispersion relations predict

$$\alpha_\pi - \beta_\pi = 5.7 \times 10^{-4} fm^3 \tag{7}$$

which is in agreement with ChPT.

To summarize the theoretical results, the $O(p^4)$ and $O(p^6)$ ChPT calculations agree on the size for $\alpha_\pi - \beta_\pi$, and they agree that $\alpha_\pi + \beta_\pi$ is small, consistent with zero. In principle the dispersion calculations can also provide a definitive prediction for the polarizabilities, however they are limited by the extrapolations used in fitting the $\gamma\gamma \to \pi^+\pi^-$ data set into the meson resonance region. The calculation by Fil'kov predicts a value for $\alpha_\pi - \beta_\pi$ twice that of ChPT, and the calculation by Pasquini is in agreement with ChPT.

4 Pion polarizability and Standard Model corrections to $g_\mu - 2$

It is well known that there is a significant difference, 3.6σ , between the E821 experimental value for muon $g_\mu - 2$ and the standard mode (SM) prediction. The errors in $(g_\mu - 2)/2$ are approximately 63×10^{-11} for experiment , and 49×10^{-11} for theory. Since the next generation $g_\mu - 2$ experiment at FNAL will reduce the experimental error by a factor of four, it is very important to reduce the SM error by a similar factor. The two largest uncertainties in the SM prediction are from hadronic vacuum polarizaton and hadronic light-by-light (HLBL) scattering. In a recent preprint Ramsey-Musolf and collaborators report that an omitted contribution to HLBL from the pion polarizability is substantial and potentially significant [En12]. Work is continuing on this important problem.

5 Measurements of the charged pion polarizability

Three different experimental techniques that have been utilized to measure α_π and β_π.

- Radiative pion photoproduction, $\gamma p \to \gamma' \pi^+ n$, at very low momentum transfer to the recoil nucleon. This reaction can be visualized as Compton scattering off a virtual pion. At forward Compton angles the reaction is sensitive to $\alpha_\pi + \beta_\pi$, and at backward angles $\alpha_\pi - \beta_\pi$. The most recent measurement has been from Mainz [Ah05] . Using the constraint $\alpha_\pi = -\beta_\pi$ they obtained

$$\alpha_\pi - \beta_\pi = 11.6 \pm 1.5_{stat} \pm 3.0_{sys} \pm 0.5_{model} \times 10^{-4} fm^3 \qquad (8)$$

  Combining errors in quadature gives 3.4 in the standard units, which differs by 1.7σ from the ChPT prediction.

- Primakoff effect of scattering a high energy pion in the Coulomb field of a heavy nucleus, $\pi A \to \pi' \gamma A$. This reaction is equivalent to Compton scattering a nearly real photon off the pion. The most recent measurement has been from Serpukov [An83] . Using the constraint $\alpha_\pi = -\beta_\pi$, they obtained

$$\alpha_\pi - \beta_\pi = 13.6 \pm 2.8_{stat} \pm 2.4_{sys} \times 10^{-4} fm^3 \qquad (9)$$

  Combining errors in quadrature gives 3.7 in the standard units, differing by 2.1σ from the ChPT prediction. The COMPASS collaboration at CERN has also taken data, and analysis is underway.

- $\gamma\gamma \to \pi^+\pi^-$. By crossing symmetry (exchanging s and t variables in the scattering amplitude) the $\gamma\gamma \to \pi\pi$ amplitude can be related to the $\gamma\pi \to \gamma\pi$ amplitude. For the $\gamma\gamma \to \pi\pi$ reaction , the sensitivity to the polarizabilities goes as $\alpha_\pi - \beta_\pi$. Babusci et al. [Ba92] used chiral perturbation theory with a one-loop correction to derive a formula they used to obtain pion polarizabilites from $\gamma\gamma \to \pi^+\pi^-$ data. Examining data sets from PLUTO, DM1, DM2, and MARK II , they obtained values of $\alpha_\pi - \beta_\pi$ ranging from 52.6 ± 14.8 in the standard units (from DM2) to 4.4 ± 3.2 (from MARK II).

To summarize the experimental data, it is difficult to draw definite conclusions from the experimental results for $\alpha_\pi - \beta_\pi$. It is generally recognized that the most model independent technique to measure hadron polarizabilities is through Compton scattering. The two most recent Compton measurements

at Serpukov (Primakov) and Mainz (virtual pion) agree that the value for $\alpha_\pi - \beta_\pi$ is approximately twice the size predicted by ChPT, albeit with large errors. The data are also in agreement with the dispersion calculation by Fil'kov. New data from Compass are especially welcome to help resolve the situation.

Turning now to the $\gamma\gamma \to \pi^+\pi^-$ data, the analysis by Babusci [Ba92] was limited by data sets with low statistics (MARK-II) and large systematic errors (see comments by Pennington in [Mo87]). It was also limited by the theoretical model, which was only one-loop in ChPT. Since then, considerable theoretical progress has been make in calculating $\gamma\gamma \to \pi\pi$ cross sections; (i) Gasser et al. [Ga06] performed a two-loop calculation in ChPT , (ii) Donoghue and Holstein [Do93] established a connection between dispersiion theory and ChPT by matching the low-energy chiral amplitude with the dispersion treatment, and (iii) Pasquini et al. [Pa08] performed a purely dispersiive treatment for the cross section.

Fig. 1 shows predicted total cross sections from Pasquini et al. for $\gamma\gamma \to \pi^+\pi^-$ for $|cos\theta_{\pi\pi}| < 0.6$. The red curve is the Born approximation calculation with no polarizability effect. The black solid curve is an unsubtracted dispersion relation (DR) calculation with $\alpha_\pi - \beta_\pi = 5.7$, and the dashed curve is the subtracted DR calculation with the same polarizability. The dotted curve is the subtracted DR calculation with the polarizabilities from [Fi06] with $\alpha_\pi - \beta_\pi = 13.0$. Comparision of the subtracted DR curves with $\alpha_\pi - \beta_\pi$ equal to 5.7 (dashed) and 13.0 (dotted), shows a change in the peak cross section at $W_{\pi\pi} \approx 0.3$ GeV of approximately 10 percent. We conclude that measurements of the pion polarizability through the $\gamma\gamma \to \pi^+\pi^-$ reaction will need statistical and systematic accuracies at the level of a few percent.

The experimental data in the figure are from MARK-II [Bo92], *where there are probably less than 400 events in the region of interest, $W_{\pi\pi} < 0.5$ GeV.* The figure clearly shows that the MARK-II data do not have the statistical precision, nor the coverage in $W_{\pi\pi}$, to provide a useful constraint on $\alpha_\pi - \beta_\pi$. It is useful to quote Donoghue and Holstein [Do93] here, " *We conclude that although $\gamma\gamma \to \pi^+\pi^-$ measurements certainly have the potential to provide a precise value for the pion polarizability, the statistical uncertainty of the present values does not allow a particularly precise evaluation.*"

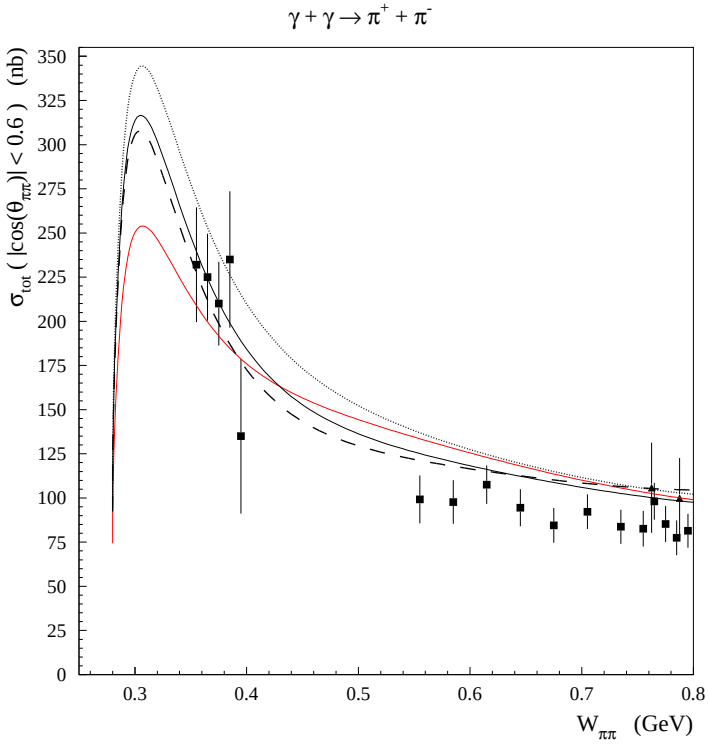

Figure 1: $\gamma\gamma \to \pi^+\pi^-$ cross sections. Red curve: Born approx. (no polarizability effect); black solid: unsubtracted DR calculation with $\alpha_\pi - \beta_\pi = 5.7$; dashed: subtracted DR with $\alpha_\pi - \beta_\pi = 5.7$; dotted: subtracted DR with $\alpha_\pi - \beta_\pi = 13.0$.

6 Measurements of the charged pion polarizability at Jefferson Lab Hall D

We propose to make measurements of $\gamma\gamma \to \pi^+\pi^-$ cross sections via the Primakoff effect using the GlueX detector in Hall D. Starting from the Primakoff result for cross sections with incident *linearly polarized photons* [Gl61] and then generalizing for a two-body final state gives,

$$\frac{d^3\sigma}{d\Omega^{Lab}_{\pi\pi} d\Omega^{CM}_{\pi} dW_{\pi\pi}} = \frac{d^2\Gamma(\gamma\gamma \to \pi^+\pi^-)}{d\Omega^{CM}_{\pi} dW_{\pi\pi}} \frac{8\alpha Z^2}{W^3_{\pi\pi}} \frac{\beta^3 E^4_{\gamma}}{Q^4} |F_{EM}(Q)|^2 sin^2\theta_{\pi\pi}(1+P_{\gamma} cos 2\phi_{\pi\pi}) \tag{10}$$

where the differential radiative width (rate) for $\gamma\gamma \to \pi^+\pi^-$ is given by

$$\frac{d^2\Gamma(\gamma\gamma \to \pi^+\pi^-)}{d\Omega^{CM}_{\pi} dW_{\pi\pi}} = \frac{d\sigma(\gamma\gamma \to \pi^+\pi^-)}{d\Omega^{CM}_{\pi}} \frac{W_{\pi\pi} k^{CM}_{\pi}}{8\pi^2} \tag{11}$$

In these expressions, $\Omega^{Lab}_{\pi\pi}$ is the lab solid angle for the emission of the $\pi\pi$ system, Ω^{CM}_{π} is solid angle for the emission of the π^+ in the $\pi\pi$ CM frame, $W_{\pi\pi}$ is the $\pi\pi$ invariant mass, Z is the atomic number of the target, β is the velocity of the $\pi\pi$ system, E_{γ} is the energy of the incident photon, $F_{EM}(Q)$ is the electromagnetic form factor for the target with FSI corrections applied, $\theta_{\pi\pi}$ is the lab angle for the $\pi\pi$ system, $\phi_{\pi\pi}$ is the azimuthal angle of the $\pi\pi$ system relative to the incident photon polarization, and k^{CM}_{π} is the momentum of the π^+ in the CM frame. Assuming a 5 percent radiation length lead target, tagged 8.5 GeV photons at a rate of 10^7 photons/s, and a running time of 500 hours, *then approximately 36,000 $\pi^+\pi^-$ Primakov events are produced in the near threshold region up to $W_{\pi\pi} = 0.5$ GeV.*

The largest physics background is from coherent ρ^0 photo-production on the nuclear target. In the helicity frame (described in Fig. 2) the angular distribution of the pions is given by [Ba72]

$$\frac{dW}{dcos\theta d\phi} = \frac{3}{8\pi} sin^2\theta_{\pi}(1 + P_{\gamma} cos 2\Psi) \tag{12}$$

where Ψ is the azimuthal angle in the helicity frame relative to the photon polariation. The differential cross section for ρ^0 photo-production on nuclear targets is given by,

$$\frac{d\sigma}{dt} = \sigma(0) e^{At} \tag{13}$$

Other important backgrounds result from nuclear coherent production of $\pi^+\pi^-$, and the nuclear incoherent production. It can be expected that the

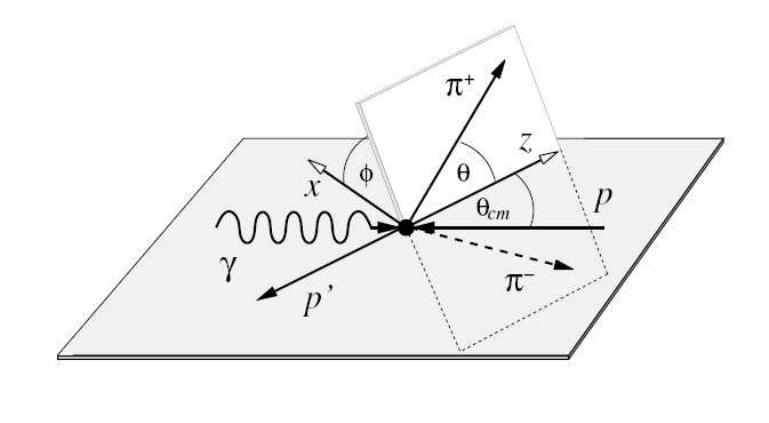

Figure 2: Diagram of the helicity frame for two pion photo-production on the nucleon

nuclear coherent production will be small compared to coherent ρ^0 production for two reasons. First, a nuclear target, specifically lead, acts as a filter to remove nuclear coherent events. This effect is clearly seen in the π^0 angular distributions measured by the PRIMEX experiment for carbon and lead [La11], and the effect will be even stronger for $\pi\pi$ final states. Because Primakoff production occurs approximtely 100 fm from the nucleus, FSI has a relatively weak effect on the Primakoff process even for heavy nuclei [Mi11]. Secondly, there should be little strength for 0^+ $\pi\pi$ production in the near threshold region resulting from $\gamma N \rightarrow f_0(600)N$. An analysis of $\pi^+\pi^-$ photoproduction at 4.7 GeV using linearly polarized photons did not see evidence for this background [Ba72].

Nuclear incoherent production can result from final state interactions of coherently produced ρ^0 mesons with the nucleus. We are collaboratiing with T. Rodrigues, who did the nuclear incoherent calculations for PRIMEX, on a similar calculation for this experiment [Ro10].

Histograms of Primakoff and coherent ρ^0 photo-production production with the event weighting given by Eqns. 10, 11, 12 , and 13 are shown in Figs. 3, 4, 5, 6, 7, and 8 . The $W_{\pi\pi}$ distribution for ρ^0 events is taken from a Zeus analysis of high-t ρ^0 photo-production on the proton [Br99]. The parameters $\sigma(0)$ and A in Eqn. 13 are taken from references [Al70] and [As67], respectively.

Fig. 3 shows the 2π invariant mass distribution for Primakoff and ρ^0 events up to a cutoff at $W_{\pi\pi} = 0.40$ GeV. The colors in the figure reference different regions in $W_{\pi\pi}$, blue is for events with $0.28 < W_{\pi\pi} < 0.32$ GeV, green is for events with $0.32 < W_{\pi\pi} < 0.36$ GeV, and red is for events with $0.36 < W_{\pi\pi} < 0.40$ GeV. Fig. 4 shows how the strength of the Primakoff process depends on $W_{\pi\pi}$. In the blue region of Fig. 3 the Primakoff process dominates; in the red region ρ^0 photo-production dominates; and in the green region the Primakoff and VMD strengths are approximately equal. The kinematic values shown in figures 5-8 illustrate their dependance on $W_{\pi\pi}$ using this same color scheme.

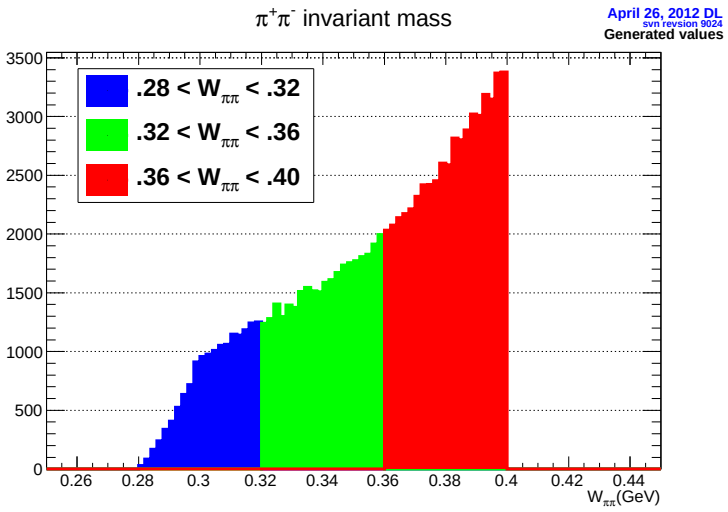

Figure 3: Histogram of $W_{\pi\pi}$ for Primakoff and ρ^0 events

Fig. 5 is the t distribution of the events. The blue curve (primarily Primakoff) shows the characheristic peaking of the Primakoff process at very low angles [Mi11]. The red curve (primarily ρ^0) is much flatter at low t , as expected by Eqn. 13.

Fig. 6 is the distribution of azimuthal angles of the $\pi^+\pi^-$ system in the lab frame, where the angle $\phi_{\pi\pi}$ is measured relative to the incident photon polarizaton direction. The blue curve (primarily Primakoff) shows a prominent $(1 - cos2\phi_{\pi\pi})$ characteristic from Eqn. 10, and the red curve (primarily ρ^0) is nearly flat.

Fig. 7 is the distribution of $\cos\theta_{\pi^+}$ in the helicity frame. The blue curve

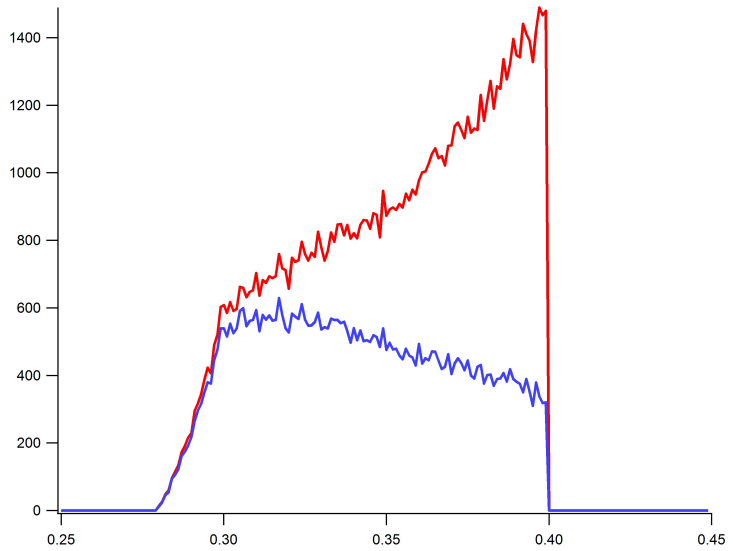

Figure 4: Histogram of $W_{\pi\pi}$ for Primakoff (blue curve) and Primakoff + ρ^0 events (red curve) events

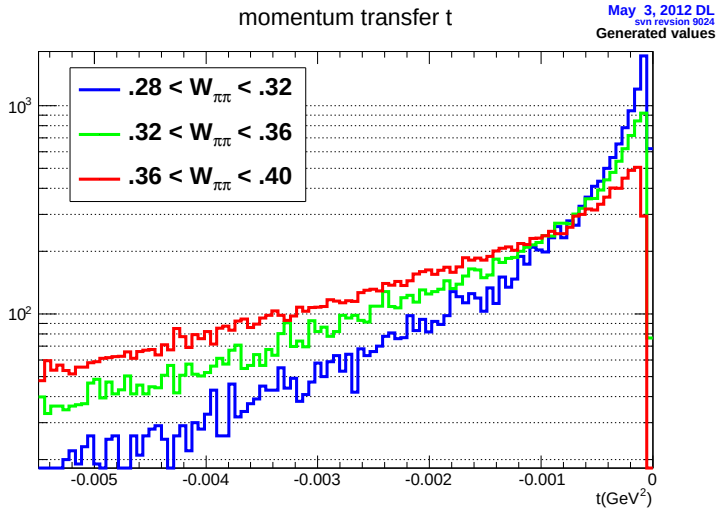

Figure 5: Histogram of t for Primakoff and ρ^0 events. The blue curve is for events with $0.28 < W_{\pi\pi} < 0.32$ GeV, green is for events with $0.32 < W_{\pi\pi} < 0.36$ GeV, and red is for events with $0.36 < W_{\pi\pi} < 0.40$ GeV.

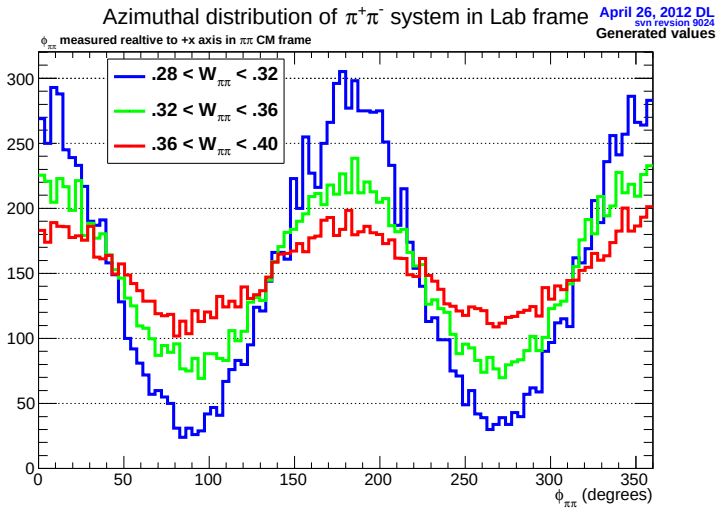

Figure 6: Histogram of $\phi_{\pi\pi}$ for Primakoff and ρ^0 events . The blue curve is for events with $0.28 < W_{\pi\pi} < 0.32$ GeV, green is for events with $0.32 < W_{\pi\pi} < 0.36$ GeV, and red is for events with $0.36 < W_{\pi\pi} < 0.40$ GeV.

(primarily Primakoff) is nearly flat because the threshold Primakoff pions are in s-waves . The red curve (primarily ρ^0) shows the $\sin^2\theta_\pi$ peaking from Eqn. 12 .

Fig. 8 is the distribution of azimuthal angles of the π^+ in the helicity frame, where the angle ψ is measured relative to the incident photon polarizaton direction. The blue curve (primarily Primakoff) is nearly flat. The red curve (primarily ρ^0) shows a prominent $(1 - cos2\psi)$ characteristic from Eqn. 12.

Based on the sensitivity of the reaction process demonstrated in these figures to incident linearly polarized photons , we estimate that it will be possible to separate contributions from the Primakoff process from coherent ρ^0 photoproduction by measuring (i) the t distribution of the pion pairs, (ii) the azimuthal distribution of the $\pi^+\pi^-$ system in the lab frame relative to the photon polarization ($\phi_{\pi\pi}$) , and (iii) the azimuthal distribution of π^+ in the helicity frame relative to the photon polarization (ψ) . Plans for the Hall D photon source call for a peak in the coherent bremstrahlung at an energy of 8.5 to 9.0 GeV, with a photon polarization of approximately 40 percent.

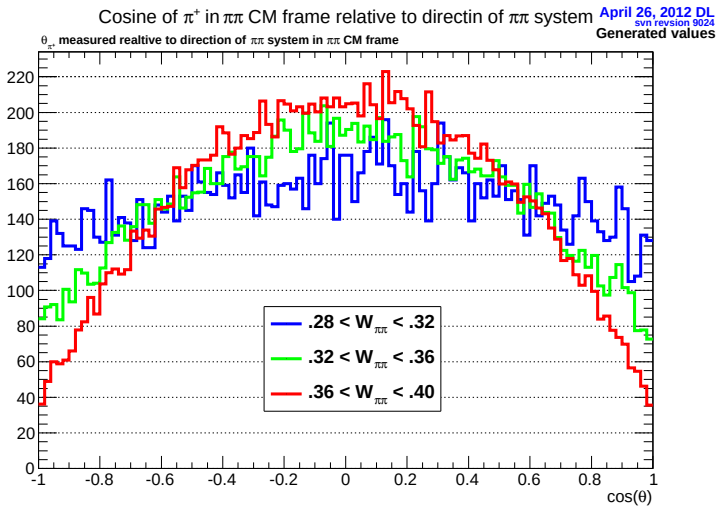

Figure 7: Histogram of $\cos\theta_{\pi^+}$ in the helicity frame for Primakoff and ρ^0 events . The blue curve is for events with $0.28 < W_{\pi\pi} < 0.32$ GeV, green is for events with $0.32 < W_{\pi\pi} < 0.36$ GeV, and red is for events with $0.36 < W_{\pi\pi} < 0.40$ GeV.

7 Simulation

The simulation effort to support this measurement is just beginning. The standard GlueX simulation and reconstruction software $sim-recon$ is being used. The simulation is done using GEANT3 and has a detailed description of the geometry (fig. 9 shows a diagram of the GlueX detector). Hits generated by the simulation are smeared using known detector resolutions. Full reconstruction is done using only the hits. This includes track finding and track fitting using a Kalman filter tracking program developed for GlueX.

Fig. 10 shows a histogram of θ_{π^+} for reconstructed π^+ tracks that start at the standard target position. For the purposes of this study, the 30cm LH_2 GlueX target was replaced with a 5% rad. len. Pb target to better represent the conditions being considered for this measurement. The single track acceptance above 1^o, the approximate low angle cutoff for the forward drift chambers (FDC's), is approximately 50 % in this preliminary study. To optimize the acceptance for low mass pion pairs, we are considering moving the target approximately 1 m upstream from the nominal target position.

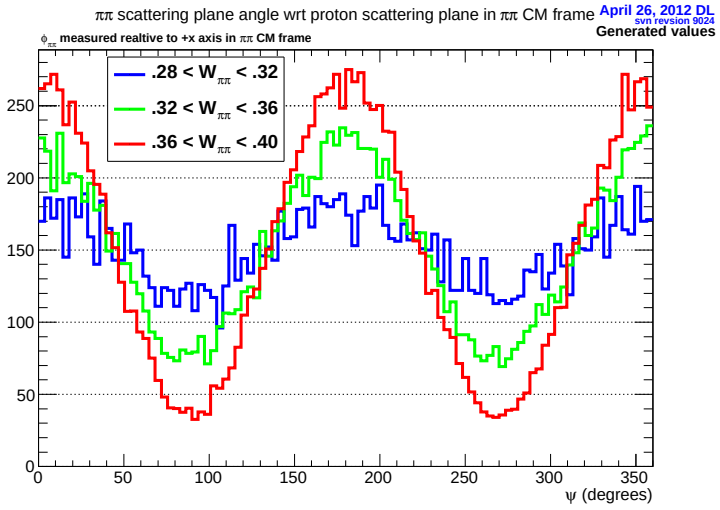

Figure 8: Histogram of ψ for Primakoff and ρ^0 events . The blue curve is for events with $0.28 < W_{\pi\pi} < 0.32$ GeV, green is for events with $0.32 < W_{\pi\pi} < 0.36$ GeV, and red is for events with $0.36 < W_{\pi\pi} < 0.40$ GeV.

This should improve the acceptance for very forward going pions to reach the FDC's in GlueX.

Future work planned for the development of a proposal includes:

- Calculation of acceptance and resolutions in $W_{\pi\pi}$, t , $\phi_{\pi\pi}$, $\cos\theta_\pi$ and ψ
- Optimizing the acceptance and resolution with respect to the target position
- Event simulation with electromagnetic and hadronic backgrounds
- Optimizing the incident photon energy, degree of linear polarization,photon rate, and acceptance for this measurement
- Detailed estimate for the experimental uncertainies in measuring $\alpha_\pi - \beta_\pi$

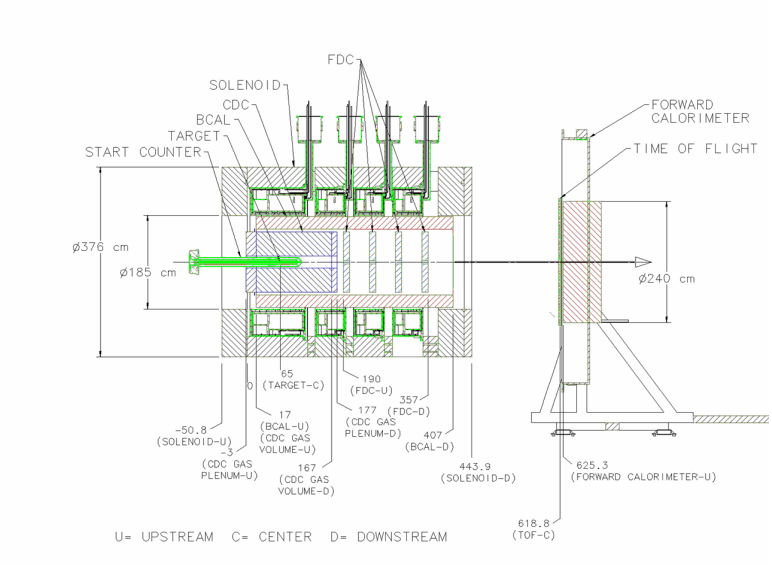

Figure 9: Diagram of the GlueX detector

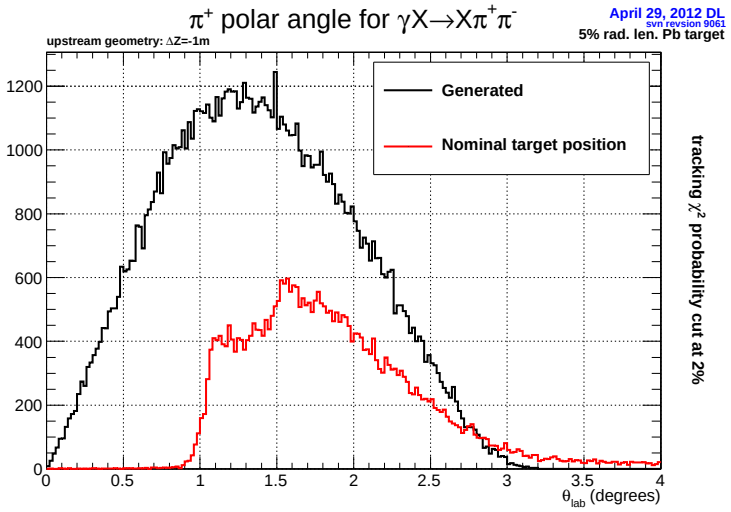

Figure 10: Histogram of θ_{π^+} for accepted π^+ tracks

8 Summary and outlook

The physics of hadron polarizabilities remains very compelling, not only as a test of theoretical calculations, but also because of the clear connection to

the science of dielectric materials. The pion polarizability plays a particularly important role in low energy tests of QCD because it directly probes the chiral-even sector of the theory. The PRIMEX result for the $\pi^0 \to \gamma\gamma$ radiative width (chiral anomaly) probed the chiral-odd sector of the theory. The most recent and arguably most accurate measurement for the pion polarizability found a value for $\alpha_\pi - \beta_\pi$ twice the size predicted by ChPT.

We can expect that new measurements of the charged pion polarizability will emerge from COMPASS, and possibly BES-III [De11] in the next few years. In the case of COMPASS this is truly a complementary technique. COMPASS will use Primakoff production with a charged pion beam (effectively Compton scattering off the pion), which has its own unique set of experimental and theoretical challenges. In the case of BES-III, to measure $\gamma\gamma \to \pi^+\pi^-$ cross sections it will be necessary to tag both of the scattered electrons, and then detect charged pions with lab kinetic energies ranging from 10 MeV to 100 MeV with a detector designed for colliding beam physics.

The theoretical tools now available for the analysis of the $\gamma\gamma \to \pi^+\pi^-$ data are greatly advanced compared to the pioneering work of Pennington [Pe92] and Babuski et al. [Ba92]. However, data with much improved statistics and sytematic uncertainties compared to MARK-II will be required to deliver a reliable measurement of $\alpha_\pi - \beta_\pi$. We estimate that statistical and systematic errors in the $\gamma\gamma \to \pi^+\pi^-$ cross sections should be at the level of a few percent, comparable to what PRIMEX achieved in its cross section measurements.

Jefferson Lab is uniquely well suited for measurements of $\gamma\gamma \to \pi^+\pi^-$ by the Primakoff effect. Hall D will have an intense flux of linearly polarized photons, and as shown in the figures in this LOI, linear polarizabation will play a key role in separating Primakoff production from the ρ^0 and other backgrounds. The GlueX detector is well suited for this measurment, having forward drift chambers for tracking and momentum measurment, and forward scintillators and calorimetry for particle ID. Finally, we note that two of the PI's on this LOI, Lawrence and Miskimen, were actively involved on the PRIMEX Primakoff experiment, with Miskimen as one of the co-spokespersons. Most of the core group from PRIMEX has moved into Hall D, working on a variety of projects. The level of experience in doing precision Primakoff experiments on nuclear targets is quite high among this group.

References

[Ah05] J. Ahrens et al., Eur. Phys. J. A23, 113 (2005).
[Al70] H. Alvensleben et al., Phys. Rev. Lett. 24, 786 (1970).
[An83] Yu. M. Antipov et al., Phys. Lett. B121, 445 (1983).
[As67] J. Asbury et al., Phys. Rev. Lett. 19, 865 (1967)
[Ba72] J. Ballam, et al., Phys Rev D 5, 545 (1972).
[Ba92] D. Babusci, et al. Phys. Lett. B 277, 158 (1992).
[Bo92] J. Boyer et al. (MARK-II collaboration), Phys. rev. D 42, 1350 (1990).
[Br99] J. Bretweg et al., arxiv:hep-ex/9910038v1 (1999).
[Bu96] U. Burgi, Nucl. Phys. B479, 392 (1996)
[By09] M. Bychkov et al., Phys. Rev. Lett., 103, 051802 (2009).
[De11] Private communication, A. Denig (2011).
[Do89] J. F. Donoghue and B. Holstein, Phys. Rev. D 40, 2378 (1989).
[Do93] J. F. Donoghue and B. R. Holstein, Phys. Rev. D 48, 137 (1993).
[En12] K. Engel, H. Patel, M. Ramsey-Musolf, arXiv:1201.0809v2 [hep-ph]
[Fi06] L.V. Fil'kov and V.L. Kashevarov, Phys. Rev. C 73, 035210 (2006).
[Ga84] J. Gasser and H. Leutwyler, Ann. Phys. 158, 142 (1984).
[Ga06] J. Gasser, M.A. Ivanov, and M. E. Sainio, Nucl. Phys. B745, 84 (2006).
[Gl61] V. Glaser, and R. A. Ferrell, Phys. Rev. 121, 886 (1961).
[Ho90] B. Holstein, Comm. Nucl. Part. Phys. 19, 221 (1990)
[Ho92] B. Holstein, Nucl. Phys. A546, 213 (1992).
[La11] I. Larin et al., Phys. Rev. Lett. 106, 162303 (2011).
[Mi11] R. Miskimen, Ann. Rev. Nucl. and Part. Sci., 61, 1 (2011)
[Mo87] D. Morgan and M.R. Pennington, Phys. Lett. B 192 (1987).
[Pa08] B. Pasquini, D. Drechsel, and S. Scherer, Phys. Rev. C 77, 06521 (2008).
[Pe92] see M.R. Pennington, in DAΦNE Physics Handbook, ed. L. Maiani, G.Pancheri and N. Paver (INFN, Frascati, 1992) and references therein.
[Ro10] T. Rodrigues et al., Phys. Rev. C 82, 024608 (2010).
[Sc05] M. Schumacher, Prog. Part. and Nucl. Phys. 55, 567 (2005).
[We71] J. Wess and B. Zumino, Phys. Lett. 37B, 422 (1971), and E. Witten, Nucl. Phys. B223, 422 (1983).